Korea-Australia Rheology Journal
Vol. 14, No. 1, March 2002 pp. 25-32

Polyethylene flow prediction with a differential multi-mode Pom-Pom model

R.P.G. Rutgers*, N. Clemeur, S. Muke[1] and B. Debbaut[2]
Department of Chemical Engineering, University of Queensland St Lucia, Queensland 4072, Australia
[1]Department of Chemical and Metallurgical Engineering, RMIT University, Melbourne Victoria, Australia 3001
[2]Polyflow s.a., Louvain-la-Neuve, Belgium

(received Ocober 23, 2001; final revision received February 11, 2002)

Abstract

We report the first steps of a collaborative project between the University of Queensland, Polyflow, Michelin, SK Chemicals, and RMIT University, on simulation, validation and application of a recently introduced constitutive model designed to describe branched polymers. Whereas much progress has been made on predicting the complex flow behaviour of many - in particular linear - polymers, it sometimes appears difficult to predict simultaneously shear thinning and extensional strain hardening behaviour using traditional constitutive models. Recently a new viscoelastic model based on molecular topology, was proposed by McLeish and Larson (1998). We explore the predictive power of a differential multi-mode version of the pom-pom model for the flow behaviour of two commercial polymer melts: a (long-chain branched) low-density polyethylene (LDPE) and a (linear) high-density polyethylene (HDPE). The model responses are compared to elongational recovery experiments published by Langouche and Debbaut (1999), and start-up of simple shear flow, stress relaxation after simple and reverse step strain experiments carried out in our laboratory.

1. Introduction

The rheological properties of polymers depend significantly on their topology. A long-chain branched polymer exhibits a pronounced strain-hardening behaviour in extensional flow, while the elongational viscosity of a linear polymer melt hardly rises above the linear viscoelastic response. In simple shear flow however, both linear and long-chain-branched polymers show a strong shear-thinning behaviour. Complex combinations of simple shear and elongational flow are often found in industrial processing geometries, therefore, in some circumstances, a suitable constitutive equation should preferably be able to simultaneously predict the material behaviour in each type of flow. Classical integral constitutive models, such as the KBKZ class, do not allow the simultaneous prediction of strain hardening and shear thinning in all types of complex flow. And despite progress is currently being made to adapt the KBKZ model to accommodate this behaviour (e.g. Olley, 2000; Mitsoulis, 2001), the numerical treatment of such constitutive equations remains endowed with significant difficulties.

Constitutive theories have focussed on simplified representations of the actual polymer architecture, representing only the most dominant components of the topology. The very successful tube model of Doi and Edwards (1986) has been the basis of much constitutive modelling research. McLeish and Larson (1998) have extended this theory for branched polymers. The molecules are represented by a simple branched architecture consisting of two "pom-poms" of q arms each, linked by a backbone that is confined in a tube. The key feature of this constitutive model is the presence of separated relaxation mechanisms for the macromolecular orientation and stretch. To facilitate numerical computation, the integral type model has been simplified to a set of differential equations which is less demanding in terms of computation time. Although in recent papers by Rubio and Wagner (2000) and Wapperom and Keunings (2001) some discrepancies between the integral model and its differential approximation have been reported, most current research uses the differential version of the model (Inkson *et al.*, 1999; Bishko *et al.*, 1999, Blackwell *et al.*, 2000, Verbeeten *et al.*, 2001).

Inkson *et al.* (1999) have extended the model to a theoretical multi-mode model where they show very good fittings and predictions for various LPDE melts. It is claimed that the model parameters provide an insight in the underlying molecular structure. For example, the strain achieved before the filament break-up in an elongational experiment is suggested to be a constitutive property.

A modification of the original differential model was suggested by Blackwell *et al.* (2000) taking into account drag-strain coupling of the branch point. This allows the

*Corresponding author: rulander@cheque.uq.edu.au

arms to retract into the tube before the maximum stretch is achieved and leads therefore to a smoother transition for the elongational viscosity when the pom-pom molecule is fully stretched.

Öttinger (2001) analysed the thermodynamic admissibility of the pom-pom model in the framework of non-equilibrium thermodynamics. He found the pom-pom model thermodynamically admissible, but suggested a modification of the orientation relaxation that produces a non-zero second normal-stress difference. Verbeeten *et al.* (2001) have very recently proposed alterations to the model, removing the finite extensibility condition and adding a non-zero second normal stress difference. Predictions for a low and high density polyethylene were shown in close agreements with experimental data.

To date, complex flow simulation of the pom-pom model is only just starting to be investigated. Bishko *et al.* (1999) and Wapperom and Keunings (2001) performed numerical simulations of contraction and contraction/expansion flows with a single-mode model using either the differential or the integral versions of the model. Using a significant solvent viscosity (possibly to avoid numerical instabilities) Bishko *et al.* (1999) showed similarities with experimental birefringence patterns obtained for a branched polymer, although no direct comparison is made. Very recently, Lee *et al.* (2001) reported two-dimensional transient simulations of the flow in a multipass rheometer. They compared the simulated stresses with experimental birefringence data for branched and linear polymers. Although the stress pattern is found to be different for the linear and branched polymer, the agreement is only qualitative. In their paper, the authors also introduce a second modification to the original pom-pom model, by introducing a variable orientation relaxation time for decelerating flows.

In the present paper, the modified, although not including this latest modification, approximate differential version of the pom-pom model is used to characterise a commercial (long-chain branched) Low Density and (linear) High Density Polyethylene (LDPE and HDPE respectively). The HDPE studied here, although assumed to have a linear architecture, shows marked strain-hardening in extensional flow, justifying the use of a model primarily designed for long-chain branched materials.

The linear parameters of the model are selected using the linear relaxation spectrum while the non-linear parameters are identified on the basis of transient uniaxial extensional viscosity curves only. The resulting model is then utilised to predict the behaviour for rheometric experiments. Stress relaxation after single and multi-step strain deformations are predicted and compared to experimental data for the LDPE melt. Transient recovery experiments after uniaxial extension are simulated for the HDPE.

For all flow situations, the pom-pom model results are compared to the predictions obtained with a Phan Thien-Tanner model (PTT) (Phan-Thien and Tanner, 1977) whose parameters are fitted using the same experimental data as the pom-pom model as well as steady shear viscosity obtained using the Cox-Merz rule.

2. Constitutive equations

The pom-pom model, proposed by McLeish and Larson (1998) is derived from macromolecular concepts that stem from the Doi-Edwards tube model (Doi and Edwards, 1986). The molecules are represented by the simplest branched architecture, consisting of a backbone linking two "pom-poms" of q arms each. The topological constraints caused by neighbouring chains are represented by a confining tube. The chain is not allowed to move more than the tube diameter perpendicular to the tube axis, while along the tube, the pom-poms will not allow the backbone to reptate or retract as freely as a linear polymer. This last feature leads to a strong strain-hardening behaviour. In flow, the tube will be stretched and will drag the backbone with it. When a certain stretch is attained, it becomes more favorable to lose entropy by withdrawing the free ends into the tube than to continue to stretch the backbone. The requirement that Gaussian chain statistics are maintained in equilibrium implies that the maximum allowed stretch sustainable by the backbone is equal to the number of arms, q. Beyond this limit, the tension in the backbone is sufficient to withdraw the free ends into the tube. The dynamic variables involved in the description of the molecule are the dimensionless stretch ratio of the backbone $\lambda(t)$, the orientation tensor $\mathbf{S}(t)$ which measures the distribution of unit vectors along the backbone and $s_c(t)$, the dimensionless distance of arms withdrawal into the tube. McLeish and Larson (1998) have shown that the arms withdrawal into the tube only has an insignificant contribution to the stress and can therefore be ignored ($s_c(t)=0$). Thus, the main difference with other constitutive models is the separation of orientation and stretch relaxation mechanisms in the mathematical description of the model.

In order to simulate a polyethylene with molecular weight and branching distribution, a multi-mode approximate differential model proposed by Inkson *et al.* (1999) is used. This multi-modal approach describes polydisperse long chain branched molecules by a theoretical blend of pom-pom molecules with different number of arms and by assigning orientational relaxation times from the linear relaxation spectrum. The relaxations of the different segments of the long chain branched molecules are decoupled from each other. A correction suggested by Rubio and Wagner (2000) is adopted as well as a local branch-point displacement factor v_i^*, proposed by Blackwell *et al.* (2000). The following set of equations is thus used:

$$\sigma(t) = \sum_i 3g_i\lambda_i^2(t)\mathbf{S}_i(t), \tag{1}$$

$$\overset{\nabla}{\boldsymbol{A}}_i(t) + \frac{1}{\tau_{b_i}}(\boldsymbol{A}_i(t)-\boldsymbol{I}) = \boldsymbol{0}, \quad (2)$$

$$\boldsymbol{S}_i(t) = \frac{\boldsymbol{A}_i(t)}{\mathrm{trace}(\boldsymbol{A}_i(t))}, \quad (3)$$

$$\frac{D}{Dt}\lambda_i(t) = \lambda_i(t)(\nabla v:\boldsymbol{S}_i(t)) - \frac{1}{\tau_{s_i}}(\lambda_i(t)-1)e^{(v_i^*(\lambda_i(t)-1))} \quad (4)$$

strictly for $\lambda_i(t)<q_i$, $\lambda_i(t)=q_i$, otherwise

Equation (1) relates the total extra-stress tensor $\boldsymbol{\sigma}$ to the orientation tensor $\boldsymbol{S}_i$ and the backbone stretch λ_i, originating from the individual modes. The subscript i identifies the mode number. $\boldsymbol{A}_i$ is an auxiliary tensor used to obtain the tensor $\boldsymbol{S}_i$ through equation (3). Equations (2) and (4) describe the evolution of the orientation tensor and the backbone stretch respectively. The plateau moduli g_i and the backbone orientation relaxation time τ_{bi} are fitted using linear viscoelastic measurements. The non-linear parameters, determined from the transient elongational viscosity curves only, are the relaxation time for stretch τ_{si} and the number of arms q_i. The parameter v_i^* was chosen equal to $2/q_i$ as recommended for LDPE melts by Blackwell *et al.* (2000).

The pom-pom predictions are compared to a multi-mode Phan-Thien-Tanner (PTT) model (Phan-Thien and Tanner, 1977). In this model, the total extra-stress tensor $\boldsymbol{\sigma}$ also results from individual contributions σ_i, which obey the following constitutive relationship:

$$\exp\left[\frac{\varepsilon_i}{g_i}\mathrm{tr}(\sigma_i)\right]\sigma_i + \tau_i\left[\left(1-\frac{\xi_i}{2}\right)\overset{\nabla}{\sigma}_i + \frac{\xi_i}{2}\overset{\Delta}{\sigma}_i\right] = g_i\tau_i(\nabla v+\nabla v^T) \quad (5)$$

where τ_i are the relaxation times and ε_i, ξ_i are the non-linear parameters. The symbols ∇ and Δ stand for the upper- and lower-convected time derivative operators, respectively.

3. Materials and experiments

3.1. Characterisation of linear and non-linear model parameters

Two different materials were characterised and simulated in this study. The LDPE melt (referred to as LD20) of BP has a molecular weight M_w of 82995 (from GPC data) and a high polydispersity of Mw/Mn 4.94 (from GPC data). The precise molecular structure is unknown, but it is expected that a high proportion of long chain branches exists, as is typical for LDPE. The shear behaviour of the material at 180°C was characterised at The University of Queensland (UQ) and the extensional behaviour at 180°C was determined at the Royal Melbourne Institute of Technology University (RMIT). Dynamic rheometry in the linear viscoelastic domain was performed under Nitrogen on an ARES rheometer (Rheometrics Scientific) yielding the relaxation spectrum for a frequency range of 10^{-2} to 10^{2} s^{-1}.

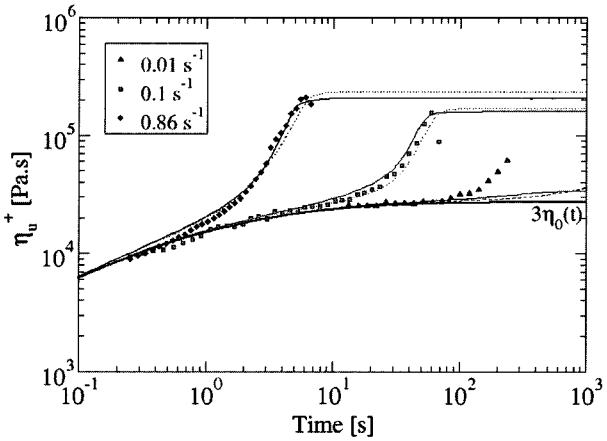

Fig. 1. Transient uniaxial extensional viscosity for the LDPE at 180°C. The symbols represent the experimental data, the continuous curves refer to the pom-pom fitting and the dotted curves to the PTT fitting.

For the LDPE the relaxation spectrum (τ_{bi}, g_i) was obtained through a downhill simplex method where the time constants are spaced evenly on the logarithmic scale. The elongational behaviour was characterised with an RME (Elongational Rheometer for Melts - Rheometric Scientific) for strain rates of 0.01, 0.1 and 0.86 s^{-1} (Figure 1) and used for the fitting of the non-linear parameters. In this Meissner-type rheometer two metal conveyor belts are used to hold the rectangular polymer sample by its extremities (Meissner, 1994). Between the conveyor belts, the sample is supported by a cushion of inert gas. The belts rotate in opposite directions and, as a result, the melt is elongated homogeneously at a constant strain rate. As observed by (Schweizer, 2000), the real strain rate applied must sometimes be corrected, in particular for high strain rate values.

The second material, a HDPE melt, is a general-purpose blow moulding resin produced by Solvay. The experimental data published and described by Langouche and Debbaut (1999) are used here and were obtained in the same manner as for the LDPE.

3.2. Characterisation of non-linear behaviour in reverse flows: reverse step-strain of LDPE

The purpose of the corresponding mathematical exercise here is to assess the predictive capability, and hence the suitability of the selected constitutive models and concepts in flow situations characterised by relatively simple and well-controlled flow kinematics, which involve reversal mechanisms. In order to evaluate the predictive capabilities of both PTT and pom-pom models for these melts, a comparison between experiment and prediction must be carried out for other flow types than those used to fit the parameters of the model. We consider a single step strain experiment (referred to as type A, analogous to Wagner, 1998) with various strain amplitudes, as well as several double

step strain experiments, as suggested by Wagner (1998). In the double step experiments, three conditions are considered. These experiments, referred to as type-B, -C and -D, start from rest state and involve a step strain of assigned amplitude γ_1 (here γ_1=4). After a specified time interval (here t=0.2 s), a reverse step strain γ_2 of $-\gamma_1/2$, $-\gamma_1$ and $-2\gamma_1$ is applied for the type-B, -C and -D experiments respectively. Not only do these experiments represent a severe test for the constitutive models, they are furthermore highly representative for the complex flow kinematics undergone by melts in industrial processes, where sequences of contraction and expansion are often met.

3.3. Characterisation of non-linear behaviour in reverse flows: transient extensional recovery of HDPE

Various types of experiments are recommended to test constitutive equations (Tanner, 2000). Amongst these, transient extensional recovery has some similarity with the reverse-step-strain experiment described above but is also a so-called strong flow, in view of its elongational character. In this type of experiment, the sample is allowed to recover freely after being stretched under well-controlled conditions. The stress relaxation is observed, as well as the transient deformation of the sample, which is no longer imposed. Transient recovery experiments were performed by Langouche and Debbaut (1999) for the HDPE melt and compared to the multi-mode PTT model predictions. In the present paper, a similar analysis is performed using the pom-pom model and the results are compared to the experimental data and the PTT model predictions.

4. Prediction of reverse step strain behaviour of LDPE

For the LDPE simulations, both pom-pom and PTT models were coded using Matlab using an algorithm adapted for stiff problems. The resulting ODE equations were solved using a third-order Runge-Kutta scheme with adaptive stepsize control. In transient extensional deformation, pronounced strain hardening was observed for both materials. The model parameters fitted to the linear viscoelastic behaviour and to the transient elongational data are listed in Table 1. The experimental extensional data as well as the fitted model response are shown in Figure 1. The agreement is very good for the strain rate of 0.86 s^{-1} and 0.1 s^{-1} but not for the strain rate of 0.01 s^{-1} probably because of the lack of linear viscoelastic data at low frequencies. A similar problem was already reported by Inkson *et al.* (1999). Since most of the experiments discussed below involve characteristic times well below the longest relaxation time, it is believed that this discrepancy at low strain rates will not significantly affect the model predictions.

To start with, we evaluate the predictive capability of the

Table 1. Parameters for the seven-mode pom-pom and Phan-Thien-Tanner (PTT) models

i	g_i[Pa]	τ_{bi} (τ for PTT) [s]	pom-pom (ν_i*=2/q_i) τ_{bi}/τ_{si}	q_i	PTT ξ_i	ε_i
1	6.282×10^{4}	1.000×10^{-2}	2	2	4.0×10^{-3}	0.129
2	1.113×10^{4}	4.641×10^{-2}	2	2	4.0×10^{-3}	0.232
3	8.760×10^{3}	2.154×10^{-1}	2	2	4.0×10^{-3}	0.114
4	2.405×10^{3}	1.000×10^{0}	2	2	1.2×10^{-2}	0.124
5	4.968×10^{2}	4.641×10^{0}	2	16	1.2×10^{-2}	0.468
6	4.662×10^{1}	2.154×10^{1}	2	20	4.0×10^{-3}	0.352
7	3.156×10^{0}	1.000×10^{2}	1.5	32	4.0×10^{-3}	0.438

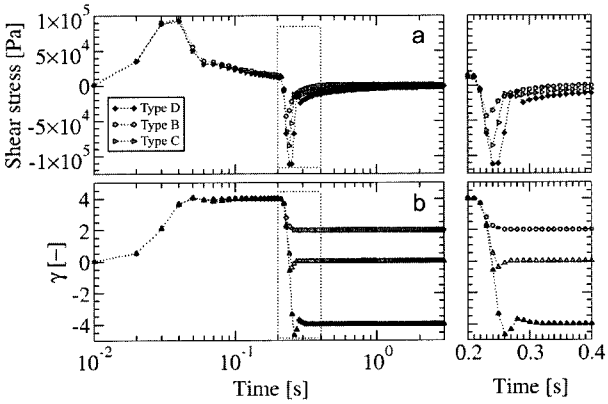

Fig. 2. Experimental stress profiles (a) and strain profiles (b) for type-B, (open circles) -C (open triangles) and -D (closed diamonds) experiments. Insert shows on a linear time scale the detail of the reverse step strain.

selected models for the LDPE melt response in single step-strain. Experiments were performed on the ARES rheometer with air-bearing actuator, with strain amplitudes of 0.1, 2 and 4. The actual imposed strain as recorded by the rheometer (rather than the ideal step-strain) was simulated to compute the stress response for both the PTT and pom-pom constitutive models. A very good agreement was found between the data and the predictions. The PTT model exhibits oscillations when approaching full relaxation, leading to negative values in the stress response within a relatively narrow interval around zero. This mechanism is a model artefact similar to the one reported by Georgiou and Vlassopoulos (1998) and Tanner (2000) for a Johnson-Segalman fluid model.

The various double-step strain experiments provide a deeper insight in the predictive performance of the model. In Figure 2(b) the strain as experimentally recorded is shown. In all cases, there is a discrepancy between the ideal step strain and the actual imposed strain: A strain growth develops during a time interval of about 0.06 s after the start of the experiment. A similar transient is found when the reverse strain is applied. Moreover, for type-C and -D experiments, the strain reversal exhibits an under-

shoot below the assigned value during a short time interval. Most probably, these experimental artefacts are in connection with the inertia of the device, and hence cannot easily be circumvented. The actual flow kinematics have therefore been considered to predict the PTT and PomPom model responses.

Figure 2(a) shows the development of the shear stress for all three double-step strain experiments. First of all, we find in all three cases an identical stress response to the first step strain: this indicates excellent repeatability of the experiments. The stress development exhibits a rapid growth in response to the applied step strain. Once the nominal strain is reached, the stress starts its decay until, at time t=0.2 s, the reverse strain is applied, and from there, different responses are expected, corresponding to the different double-step strain experiments. All three experiments are discussed below, but the model predictions are only shown graphically in Figure 3, for the most severe type-D experiment.

For the type-B experiment ($\gamma_2 = -½\gamma_1$) , once the reversal strain is applied, the stress almost instantaneously changes sign. During decay, this stress remains negative for a short time interval of less than 0.2 s. After that time, the stress becomes positive again, presumably because the stress from the original larger positive strain is still decaying in the material. A very good agreement is found between the predictions obtained with both the PTT and pom-pom constitutive models and the corresponding experimental data for the total time interval. Although both models appear to slightly over-predict the peak in the initial stress response this is attributed to the sparse experimental data due to the extremely short time interval.

In the type-C experiment ($\gamma_2 = -\gamma_1$), upon reversal of the strain a negative stress peak is obtained of almost equal magnitude to the original stress peak response to the first step strain. This stress subsequently decays monotonically to zero, without becoming positive. Again a very good agreement is found between predictions and experimental data for the total time interval for both models. The predictions with the PTT model are essentially the same as those obtained with the pom-pom model. However, the previously mentioned oscillating response of the PTT model develops after the second strain is applied, although this is actually apparent on a logarithmic plot only, i.e. the corresponding values are close to zero.

Finally, as shown in Figure 3, when the second strain is applied in the type-D experiment ($\gamma_2 = -2\gamma_1$), the stress rapidly becomes negative and exhibits similar behaviour as during the first strain, with an opposite sign. The stress remains negative until complete relaxation. A similar behaviour is predicted with the pom-pom model, which is also able to accurately render the somewhat sophisticated stress response at the instant of the strain change. At this point the PTT model performs less well in predicting the overshoot, and the predicted response is anew affected by the oscillation mechanism already mentioned above.

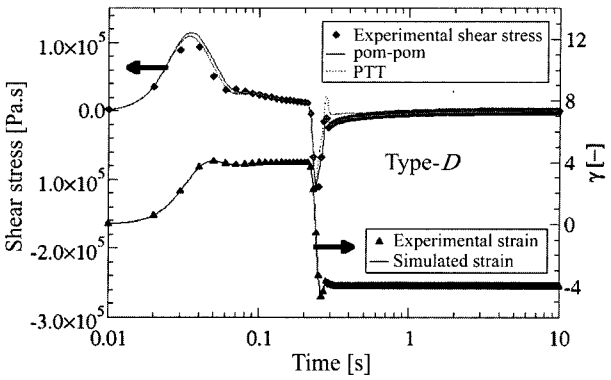

Fig. 3. Strain history and shear stress response for type-D experiments. Symbols represent experimental data, continuous curve Pom-Pom model response, dotted curve PTT response.

5. Rheometric predictions for HDPE

For the HDPE melt, a 9-mode pom-pom model was fitted to the published linear viscoelastic and uniaxial extension data. (Langouche and Debbaut, 1999). Figure 4 shows that good fits of the transient uniaxial extension data are obtained for all strain rates; thanks to the wider relaxation spectrum, a better fit is obtained at 0.01 s^{-1} than achievable for the LDPE (Figure 1). In Table 2, we report the linear and non-linear parameters that were identified for the pom-pom model. The branching parameter q_i displays a narrow distribution of low values, as expected for this predominantly linear molecular architecture. To obtain a good fitting of the uniaxial elongational properties, the recommendations given by Inkson *et al.* (1999) where not strictly followed in the selection of the other non-linear parameters

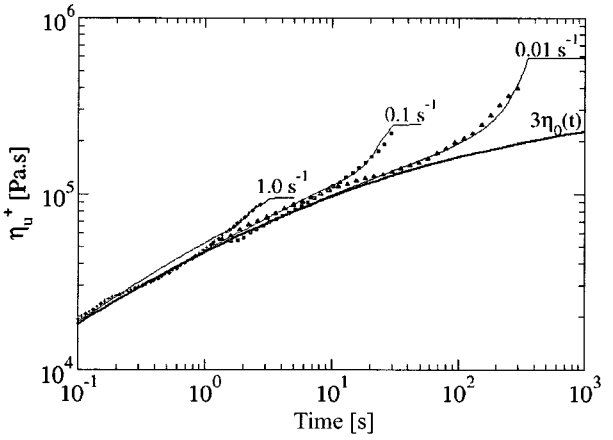

Fig. 4. Transient uniaxial extensional viscosity for the HDPE at 180°C. The symbols represent the experimental data, the continuous curves refer to the fitted pom-pom response.

Table 2. Parameters for the nine-mode pom-pom and Phan-Thien-Tanner (PTT) models

i	g_i[Pa]	τ_{bi} (τ for PTT) [s]	Pom-pom			PTT	
			τ_{bi}/τ_{si}	q_i	ν_i*	ξ_i	ε_i
1	1.803×10^5	4.495×10^{-3}	3.02	1	0.0	0.067	0.093
2	7.561×10^4	1.976×10^{-2}	3.00	1	0.0	0.065	0.565
3	3.216×10^4	8.684×10^{-2}	3.00	1	0.0	0.113	0.919
4	1.307×10^4	3.817×10^{-1}	11.7	1	0.0	0.074	0.920
5	4.876×10^3	1.678×10^{0}	28.4	1	0.0	0.142	0.271
6	1.557×10^3	7.375×10^{0}	49.2	2	1.0	0.206	0.543
7	4.822×10^2	3.241×10^{1}	10.8	4	1.0	0.246	0.146
8	7.868×10^1	1.425×10^{2}	2.28	6	1.0	0.310	0.039
9	3.573×10^1	6.262×10^{2}	3.01	6	0.3	0.531	10^{-5}

(τ_{si} and ν_i*). The parameters for the PTT model were adopted from Langouche and Debbaut (1999).

The pom-pom fitting of the linear viscoelastic data and the prediction of the steady shear behaviour is given in Figure 5. Assuming validity of the Cox-Merz rule for the experimental data, the pom-pom prediction slightly over-predicts the shear thinning behaviour of the material.

In transient elongational recovery experiments using an RME device, an initial stress state is generated by stretching the sample at a given strain rate up to a given Hencky strain. Once the desired strain is achieved, the sample is cut at one end, and its recovery is measured by recording the length L(t) using video equipment. In order to predict the response in terms of the strain, an explicit pom-pom equation in terms of strain as a function of stress and strain history must be formulated.

The recovery after elongation occurs in two stages: At time t_0 the material undergoes an instantaneous recovery resulting in an instantaneous change in strain E.

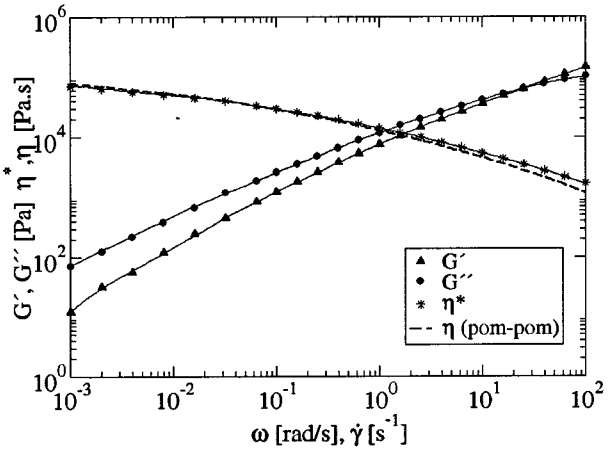

Fig. 5. Linear viscoelastic and steady shear behaviour of HDPE. Symbols represent experimental data; continuous curves the fitted Pom-Pom linear viscoelastic behaviour; dashed curve the predicted steady shear pom-pom response.

At t_0 the strain rate and strain become $\dot{\varepsilon} = E\delta(t-t_0)$ and $\varepsilon = \varepsilon_{0^-}+E$ respectively, which yields for the components of the auxiliary tensor **A** (the subscript i is momentarily omitted for sake of clarity):

$$A_{11}(t_{0^+}) = A_{11}(t_{0^-})e^{-E} \text{ and } A_{33}(t_{0^+}) = A_{33}(t_{0^-})e^{2E} \tag{6}$$

Assuming the affine stretch hypothesis for all modes, one can write for the backbone stretch:

$$\lambda(t_{0^+}) = \lambda(t_{0^-})\sqrt{\frac{2A_{11}(t_{0^-})e^{-E}+A_{33}(t_{0^-})e^{2E}}{2A_{11}(t_{0^-})+A_{33}(t_{0^-})}} \tag{7}$$

Assuming that the stresses become isotropic (i.e. $\sigma_{11}(t_{0^+}) = \sigma_{33}(t_{0^+})$) as a result of the instantaneous recovery, it is possible to solve for the instantaneous change in strain E using the known state obtained at the end of the elongation. $S^+_{11_i}$, $S^+_{33_i}$ and λ_i^+ are determined using (6) and (7).

Afterwards, a natural recovery occurs where the material tends to slowly recover towards its original shape. Equation (2) and equation (4) become, respectively:

$$\frac{dA_{11}}{dt} + \left(\dot{\varepsilon}+\frac{1}{\tau_b}\right)A_{11} = \frac{dA_{33}}{dt} - \left(2\dot{\varepsilon}-\frac{1}{\tau_b}\right)A_{33} = \frac{1}{\tau_b} \text{ and } A_{22}=A_{11} \tag{8}$$

$$\frac{d\lambda}{dt} = \lambda\dot{\varepsilon}(S_{33}-S_{11}) - \frac{1}{\tau_s}(\lambda-1)e^{\nu^*(\lambda-1)} \tag{9}$$

During this second phase a vanishing total elongational stress difference is assumed:

$$\frac{d}{dt}(\sigma_{33}-\sigma_{11}) = \sum_i \frac{d}{dt}\left(\frac{3g_i\lambda_i^2(A_{33i}-A_{11i})}{A_{33i}+2A_{11i}}\right) = 0 \tag{10}$$

These equations can be rewritten into an explicit expression for the strain rate:

$$\dot{\varepsilon}(t) = \frac{\Sigma_i \dfrac{2\lambda_i g_i(A^i_{33}-A^i_{11})(\lambda_i-1)\exp(\nu_i^*(\lambda_i-1))}{\tau_{si}(A^i_{33}+2A^i_{11})} + \dfrac{3\lambda_i^2 g_i(A^i_{33}-A^i_{11})}{\tau_{bi}(A^i_{33}+2A^i_{11})^2}}{\Sigma_i \dfrac{2\lambda_i^2 g_i(A^i_{33}-A^i_{11})^2}{(A^i_{33}+2A^i_{11})^2} + \dfrac{9\lambda_i^2 g_i(A^i_{33}A^i_{11})}{(A^i_{33}+2A^i_{11})^2}} \tag{11}$$

To deal with the large number of time steps involved in the recovery simulation, a C^{++} program was developed. The recovery factor (i.e. the ratio of the current length $L(t)$ over the initial sample length L_0 after stretch) is plotted in Figure 6 for various extension histories. Predictions of the pom-pom model are in good agreement with experimental data for moderate strain rate. The pom-pom prediction slightly overestimates the recovery after extension with a Hencky strain of 2 and a strain rate of 1. The usual experimental sources of error may explain this. In addition, as suggested by Langouche and Debbaut (1999), an irrevers-

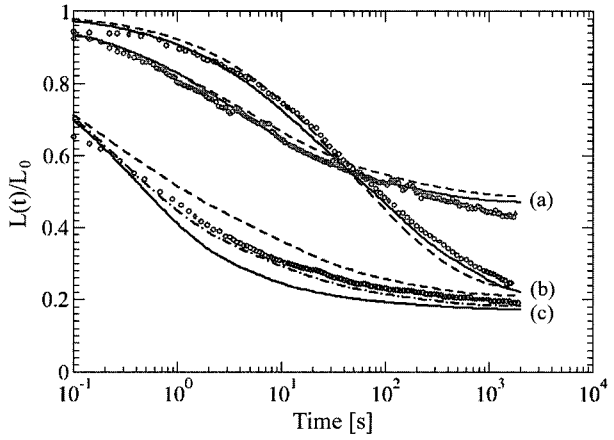

Fig. 6. Recovery factor $L(t)/L_0$ versus time for recovery experiments performed at several Hencky strains and strain rates: (a) strain = 3; strain rate = 0.01, (b) strain = 1; strain rate = 0.1 and (c) strain = 2; strain rate = 1. The symbols represent the experimental data, the continuous curve the pom-pom prediction and the dotted curve the PTT prediction. The dash-dotted line represents the pom-pom prediction with the modified orientation relaxation time (Lee *et al.*, 2001).

ible mechanism of molecular disentanglement due to high deformation undergone by the melt sample during extension may possibly be the origin of this deviation. Also, it is possible that the presently selected model is not endowed with the best irreversible mechanism that would be needed in some situations. At this point it is interesting to take the recent modification of the pom-pom model (Lee *et al.*, 2001) into account in the simulation. Unfortunately, with this model, it is no longer possible to find an explicit formulation for the strain rate as in formula (11). Therefore, some iterations have to be performed for each time step in order to obtain the strain rate. Although this addition to the model has very little impact for moderate strain rate (not represented here for sake of clarity), the prediction for the higher strain rate (curve c) is clearly improved (Figure 6). Another possible explanation is that the actual strain rate achieved experimentally could be lower than 1 s^{-1}, due to slip or other experimental difficulties at such high strain rates.

The pom-pom constitutive model used here yields comparable accuracy to the PPT model used by Langouche and Debbaut (1999). This work is an early indication that the pom-pom model may be suitable to mimic the complex rheological behaviour of HDPE despite its predominantly linear topology.

6. Conclusions

The differential pom-pom model was successfully used to predict LDPE behaviour under severe reverse simple shear deformations. The predictive capabilities of the pom-pom model were shown to be comparable to, and at times more accurate than, the Phan-Thien-Tanner model. This provides a promising basis to investigate its behaviour in complex deformations such as planar contraction flow, where established models may not be easily applicable to LDPE.

The pom-pom model was furthermore shown to predict relatively well the behaviour of a particular grade of HDPE that exhibits strain hardening. It appears that despite the expected predominantly linear architecture of this polymer, its responses point at topological features that behave like branch points. Despite the encouraging results, there is room for possible improvement for applying this rheological model to weakly branched materials. Also there are still unanswered questions in connection with the mathematical formulation of the pom-pom model. Finally, the present work provides useful results for a possible validation of further improvements made to the model.

Acknowledgments

The authors thank Fluent Inc., Michelin, and SK Chemicals for funding this research. Nicolas Clemeur wishes to thank Cheng Heng Hye from Ngee-Ann University, Singapore, for his precious help in conducting simple shear rheometry at The University of Queensland, and to Andrew Chryss of RMIT University, Melbourne, for RME extensional rheometry.

References

Bishko, G.B., O.G. Harlen, T.C.B. McLeish and T.M. Nicholson, 1999, Numerical simulation of the transient flow of branched polymer melts through a planar contraction using the 'pom-pom' model., *J. Non-Newton. Fluid Mech.* **82**, 255-273.

Blackwell, R.J., T.C.B. McLeish and O.G. Harlen, 2000, Molecular drag-strain coupling in branched polymer melts, *J. Rheol.* **44**, 121-136.

Doi, M. and S.F. Edwards, 1986, The Theory of Polymer Dynamics, Oxford, Clarendon Press.

Georgiou, G.C. and D. Vlassopoulos, 1998, On the stability of the simple shear flow of a Johnson-Segalman fluid, *J. Non-Newton. Fluid Mech.* **75**, 77-97.

Inkson, N.J., T.C.B. McLeish, O.G. Harlen and D.J. Groves, 1999, Predicting low density polyethylene melt rheology in elongational and shear flows with "pom-pom" constitutive equations, *J. Rheol.* **43**, 873-896.

Lee, K., M.R. Mackley, T.C.B. McLeish, T. M. Nicholson and O.G. Harlen, 2001, Experimental observation and numerical simulation of transient "stress fangs" within flowing molten polyethylene, *J. Rheol.* **45**, 1261-1277.

Langouche, F. and B. Debbaut, 1999, Rheological characterisation of a high-density polyethylene with a multi-mode differential viscoelastic model and numerical simulation of

transient elongational recovery experiments, *Rheol. Acta* **38**, 48-64.

McLeish, T.C.B. and R.G. Larson, 1998, Molecular constitutive equations for a class of branched polymers: The pom-pom polymer, *J. Rheol.* **42**, 81-110.

Meissner, J. and J. Hostettler, 1994, A New Elongational Rheometer for Polymer Melts and Other Highly Viscoelastic Liquids., *Rheol. Acta* **33**, 1-21.

Mitsoulis, E., 2001, Numerical simulation of entry flow of the IUPAC-LDPE melt, *J. Non-Newt. Fluid Mech.* **97**, 13-30.

Olley, P., 2000, An adaptation of the separable KBKZ equation for comparable response in planar and axisymmetric flow, *J. Non-Newt. Fluid Mech.* **95**, 35-53.

Öttinger, H.C., 2001, Thermodynamic admissibility of the pom-pom model for branched polymers., *Rheol. Acta* **40**, 317-321.

Phan-Thien, N. and R.I. Tanner, 1977, A new constitutive equation derived from network theory, *J. Non-Newton. Fluid Mech.* **2**, 353-365.

Rubio, P. and M.H. Wagner, 2000, LDPE melt rheology and the pom-pom model, *J. Non-Newton. Fluid Mech.* **92**, 245-259.

Schweizer, T., 2000, The uniaxial elongational rheometer RME - six years of experience, *Rheol. Acta* **39**, 428-443.

Tanner, R.I., 2000, Engineering Rheology, Oxford, Oxford University Press.

Verbeeten, W.M.H., G.W.M. Peters and F.P.T. Baayens, 2001, Differential constitutive equations for polymer melts: The extended Pom-Pom model, *J. Rheol.* **45**, 823-844.

Wagner, M.H., P. Ehrecke, 1998, Dynamics of polymer melts in reversing shear flows, *J. Non-Newtonian Fluid Mech.* **76**, 183-197.

Wapperom, P. and R. Keunings, 2001, Numerical simulation of branched polymer melts in transient complex flow using pom-pom models., *J. Non-Newton. Fluid Mech.* **97**, 267-281.